Novel Synchronous Rectification and Receiving Power Compensation Method for WPT Only by DC Current Sensor

Daisuke Shirasaki, *Student Member, IEEE,* Toshiyuki Fujita, *Member, IEEE,* and Hiroshi Fujimoto, *Senior Member, IEEE*

***Abstract*—Dynamic wireless power transfer (WPT) can solve the shorter cruising range problem of electric vehicles. The synchronous rectification can improve the efficiency of WPT, but it costs more because it requires an expensive AC current sensor. A novel synchronous rectification method is proposed which only uses an inexpensive DC current sensor, and does not measure AC current or voltage. This method continuously searches the synchronous state by the gradient descent method and the feedforward phase jump control. This method also compensates the decreased received power caused by the deviation of the parameters. In the first part, it is explained by the equivalent circuit model that the proposed method can achieve the synchronous rectification by maximizing the DC received current. Then, the effectiveness of the proposed method in terms of the efficiency and the received power are verified in the experiment by comparing with the conventional diode rectification. The proposed method reduced the loss by 31.77% and achieve the synchronous rectification 4 times faster.**

***Index Terms*—wireless power transfer, synchronous rectification, phase-shift power modulation.**

I. Introduction

In recent years, wireless power transfer (WPT) has become widely used in the market. One of the most famous application is Qi which is used in smartphones. It adopts the electromagnetic induction type. This type is simple but has the disadvantage of not being able to deliver enough power in an environment with a large air gap [1]. Kurs *et al.* published the magnetic resonance coupling, and it has attracted a lot of attention. It can transfer large power with high efficiency even with a wide air gap or misalignment [2].

One of the applications of the magnetic resonance coupling is a wireless power supply to Electric Vehicle (EV) [3]. EVs have been widely used in response to the growing awareness of the environment in recent years. However, EVs still have problems, and they have not fully replaced the conventional Internal Combustion Engine Vehicle (ICEV). This would be due to the shorter range, higher vehicle price, and longer charging time compared to ICEV [4][5][6].

These problems can be resolved by dynamic wireless power transfer (DWPT). Power can be transferred from the road side to vehicles by installing road side coils to intersections in cities and expressway, and installing vehicle side coils to EVs [7].

D. Shirasaki, T. Fujita and H. Fujimoto are with the Department of Advanced Energy, Graduate School of Frontier Sciences, The University of Tokyo, 5-1-5, Kashiwanoha, Kashiwa city, Chiba 277-8561, Japan (TEL: +81-4-7136-3881, email: shirasaki.daisuke19@ae.k.u-tokyo.ac.jp).

There are some points to be improved for the high efficiency of the WPT. One technology is the rectifier. Rectifiers use diodes in general, but diodes lose a certain amount of energy during rectification due to their forward voltage. The synchronous rectification can reduce the loss because the voltage drop by the on-resistance in MOS-FET is lower than that by diodes [8][9]. It uses the full-bridge converter as the rectifier instead of the diode rectifier [10]. One of the conventional method is [8], and it uses AC current sensors to get the phase of the vehicle side AC current. Then the vehicle side controls the timing of its own converter to sync the phases of its AC voltage and AC current. Other method in [9] uses the voltage of vehicle side capacitor instead of AC current to sync the phases of the vehicle side AC voltage and AC current. The phase of AC current is indirectly observed by using the fact that the phase of the capacitor voltage is delayed by 90 degrees compared to AC current. These conventional methods use the information of either or both of AC voltage and current. However, AC current sensor which can measure $85\,\mathrm{kHz}$ with small phase delay is expensive, and this increases the cost of the synchronous rectification.

A new synchronous rectification method that does not need any AC current sensors is proposed [11]. This method only needs a DC current sensor, which is cheaper than AC current sensor. The controller of the vehicle side converter monitors the DC current of the vehicle side battery, and adjusts the timing of the vehicle side converter so that the receiving DC current is maximized. This method searches maximum received point by hill climbing method generally used in maximum power point tracking [12]. As the result, the vehicle side achieves the synchronous rectification state. However, this synchronous rectification method adjusts the timing of the vehicle side converter's gate signal with the fixed width, and this leads to the bottleneck to speed up the time to reach the optimal receiving point.

Another problem with the WPT is the decrease of the efficiency when the coil parameters varies. The self inductances of the coils varies due to the effect of the ferrite [13], and the effect is more prominent in the region where the coupling coefficient is small. The variation of the self inductance leads to decrease the received power. Several studies to compensate the decreased received power have been done so far. One method is to make the phase difference between the voltage and the current by the converter. It can make the reactance, and compensate the deviation of the self-inductances. Some

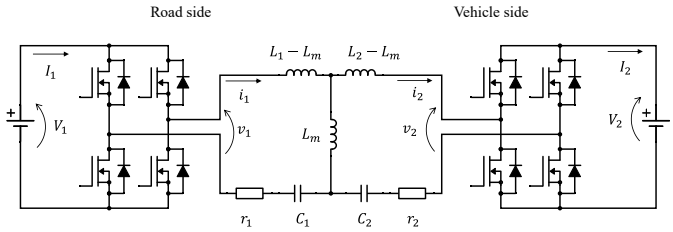

Fig. 1. Series-Series (S-S) type resonance circuit.

studies simply use full-bridge converter [14][15], and the other uses semi-brideless active rectifer to simplify the converter [16]. Another method is to insert variable capacitances made by semiconductor devices [17][18]. They compensates the deviations of parameters directly by changing the value of the variable capacitances. All of methods can compensate the deviation of the parameters, but they all use the information of AC voltage and current.

This paper introduces a novel method that can achieve both the synchronous rectification and the compensation of the decreased received power caused by the deviation of the parameters without using any AC information. This method implements the gradient descent to decide the adjustment width, and the search speed is improved compared to [11] when the optimal point is far away. A feedforward phase jump control method based on the physical properties of the coils is also implemented. Moreover, this paper elucidates that the proposed method compensates the decreased received power caused by the deviation of the parameters in the non-resonant region.

Section II introduces the principle of the proposed method. Then, Section III introduces the implementation method of the proposed method. Section IV verifies the effectiveness of the proposed method in experiments. Section V concludes that the proposed method can increase the efficiency and compensate the decreased received power caused by the deviation of the parameters.

II. PRINCIPLE OF AC SENSORLESS SYNCHRONOUS RECTIFICATION

A. Circuit Configuration

Fig. 1 shows a Series-Series (S-S) topology WPT circuit in this paper. The road side and vehicle side are connected to a DC voltage source. The road side has a full- bridge inverter, and the vehicle side has a full-bridge converter. Table I lists the meaning of each parameter in Fig. 1. Both sides drive inverters at a duty ratio of one with no pulse width modulation (PWM). The road side AC voltage $\dot{v}_1$ is described as the following equation by using the road side DC voltage V_1.

$$\dot{v}_1 = \frac{2\sqrt{2}}{\pi} V_1 \tag{1}$$

The vehicle side AC voltage $\dot{v}_2$ is described as following equition by using V_2 and the phase lead of $\dot{v}_2$ relative to $\dot{v}_1$, θ.

$$\dot{v}_2 = \frac{2\sqrt{2}}{\pi} V_2(\cos\theta + j\sin\theta) \tag{2}$$

TABLE I
MEANING AND VALUES OF THE PARAMETERS OF THE COILS

Parameter	*Meaning*	*Value*
V_1	DC Voltage of road side power-supply	70 V
V_2	DC Voltage of vehicle side battery	70 V
I_1	DC Current of road side	
I_2	DC Current of vehicle side	
v_1	AC Voltage of road side	
v_2	AC Voltage of vehicle side	
i_1	AC Current of road side	
i_2	AC Current of vehicle side	
C_1	Capacitance of road side coil	14.1 nF
C_2	Capacitance of vehicle side coil	34.5 nF
r_1	Resistance of road side coil	97.3 mΩ
r_2	Resistance of vehicle side coil	28.1 mΩ
L_1	Inductance of road side coil	248 µH
L_2	Inductance of vehicle side coil	101 µH
L_m	Mutual inductance	
k	Coupling coefficient	
θ	Phase lead of v_2 relative to v_1	
x	Distance from the center of the road side coil	

The self inductance of each coil L_1 and L_2 fluctuates with the position of the coil due to the effect of ferrite [13]. The variation are defined as ΔL_1 and ΔL_2, and L_1 and L_2 are described by using the nominal values L_{1nom}, L_{2nom}. The nominal values are the aligned conditions of the coils.

$$L_1 = L_{1nom} + \Delta L_1 \tag{3}$$

$$L_2 = L_{2nom} + \Delta L_2 \tag{4}$$

B. Proposed Method for Synchronous Rectification in the Resonant Condition

The value of capacitances in the WPT circuit is set to the resonance at operating frequency in the nominal condition. This means that ΔL_1 and ΔL_2 are zero. The circuit equations in the nominal condition are as follows.

$$\dot{v}_1 = r_1 i_1 - j\omega L_m \dot{i}_2 \tag{5}$$

$$\dot{v}_2 = -r_2 i_2 + j\omega L_m \dot{i}_1 \tag{6}$$

By solving (5) and (6) based on Kirchhoff's law, the vehicle side AC current $\dot{i}_2$ is described as the following equation.

$$\dot{i}_2 = -\frac{r_1 \dot{v}_2 - j\omega L_m \dot{v}_1}{r_1 r_2 + \omega^2 L_m^2} \tag{7}$$

By substituting (1) and (2) into (7), $\dot{i}_2$ can be described as the following equation.

$$\dot{i}_2 = -\frac{2\sqrt{2}}{\pi} \frac{r_1 V_2 \cos\theta + j(r_1 V_2 \sin\theta - \omega L_m V_1)}{r_1 r_2 + \omega^2 L_m^2} \tag{8}$$

The effective received power of the vehicle side P_2 is described as the following equation.

$$\begin{aligned} P_2 &= \mathrm{Re}(\dot{v}_2 \overline{\dot{i}_2}) \\ &= -\frac{8V_2(r_1 V_2 - \omega L_m V_1 \sin\theta)}{\pi^2(r_1 r_2 + \omega^2 L_m^2)} \end{aligned} \tag{9}$$

Thus, I_2 is described as the following equation.

$$\begin{aligned} I_2 &= \frac{P_2}{V_2} \\ &= -\frac{8(r_1 V_2 - \omega L_m V_1 \sin\theta)}{\pi^2(r_1 r_2 + \omega^2 L_m^2)} \end{aligned} \tag{10}$$

From (10), I_2 depends not only on V_1, V_2, and L_m, but also on θ. On the contrary, the communication between the road side and the vehicle side is offline, the vehicle side cannot get the value of θ. However, the vehicle side controller is able to change θ by adjusting the timing of its own converter. The switching frequencies of the road side and the vehicle side are supposed to be fixed to the resonant value. The road side just transfers power without any feedback controls. The vehicle side controller monitors the amplitude of receiver DC current I_2, and controls θ to maximize I_2. The vehicle side achieves the synchronous rectification state. I_2 is the function of θ as shown in (10).

The partial derivative of I_2 with respect to θ is described by the following equation.

$$\frac{\partial I_2}{\partial \theta} = \frac{8\omega V_1}{\pi^2(r_1 r_2 + \omega^2 L_m^2)} L_m \cos\theta \tag{11}$$

$\frac{8\omega V_1}{\pi^2(r_1 r_2+\omega^2 L_m^2)}$ is always positive, so it depends on $L_m \cos\theta$ whether $\frac{\partial I_2}{\partial \theta}$ is positive or negative. If L_m is positive, $\frac{\partial I_2}{\partial \theta}$ is positive when θ is between -90° and 90°. $\frac{\partial I_2}{\partial \theta}$ is negative for other θ. The vehicle side monitors I_2, and changes θ as to maximize I_2. As the result, θ eventually reaches 90°. When $\theta = 90^\circ$, $\dot{v}_2$ and $\dot{i}_2$ are described by the following equations.

$$\dot{v}_2 = \frac{2\sqrt{2}}{\pi} V_2 j \tag{12}$$

$$\dot{i}_2 = \frac{2\sqrt{2}}{\pi} \frac{\omega L_m V_1 - r_1 V_2}{r_1 r_2 + \omega^2 L_m^2} j \tag{13}$$

Thus, the phases of $\dot{v}_2$ and $\dot{i}_2$ are aligned when $L_m \geqq \frac{r_1 V_2}{\omega V_1}$, and the synchronous rectification is achieved.

When L_m is negative, $\frac{\partial I_2}{\partial \theta}$ is negative when θ is between -90° and 90°. $\frac{\partial I_2}{\partial \theta}$ is positive for other θ. As the result, by controlling θ to maximize I_2, θ eventually reaches -90°. When $\theta = -90^\circ$, $\dot{v}_2$ and $\dot{i}_2$ are described by the following equations.

$$\dot{v}_2 = \frac{2\sqrt{2}}{\pi} V_2 (-j) \tag{14}$$

$$\dot{i}_2 = \frac{2\sqrt{2}}{\pi} \frac{-\omega L_m V_1 - r_1 V_2}{r_1 r_2 + \omega^2 L_m^2} (-j) \tag{15}$$

The phases of $\dot{v}_2$ and $\dot{i}_2$ are aligned when $L_m \leqq -\frac{r_1 V_2}{\omega V_1}$, and the synchronous rectification is achieved.

Thus, the vehicle side achieves the synchronous rectification state in the end for k above a certain absolute value by adjusting θ to maximize I_2 in the resonant condition.

C. Effectiveness of the Proposed Method for Compensating Received Power in Non-Resonant Condition

On the other hand, $\dot{v}_1$ and $\dot{v}_2$ are described as follows in the non-resonant condition.

$$\dot{v}_1 = (r_1 + j\omega\Delta L_1) i_1 - j\omega L_m i_2 \tag{16}$$

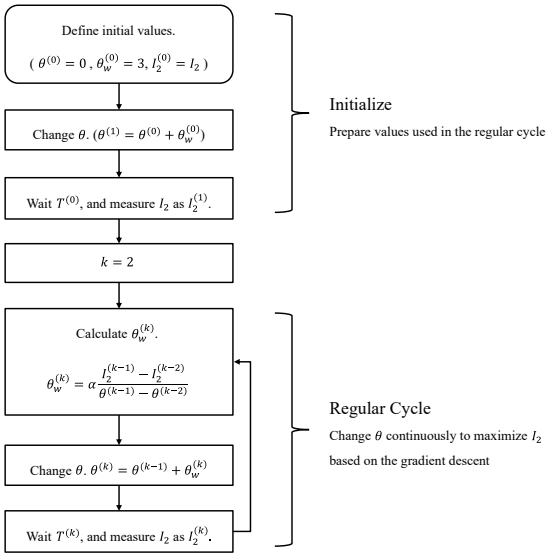

Fig. 2. Control algorithm based on gradient descent.

$$\dot{v}_2 = -(r_2 + j\omega\Delta L_2) i_2 + j\omega L_m i_1 \tag{17}$$

By solving these circuit equations, I_2 is described by the following equation at the same discussion in section II-B. A, B, C, and D are the parameters to simplify the equation.

$$A = r_1 r_2 + \omega^2 (L_m^2 - \Delta L_1 \Delta L_2) \tag{18}$$

$$B = \omega(r_1 \Delta L_2 + r_2 \Delta L_1) \tag{19}$$

$$\begin{aligned} C = \frac{2\sqrt{2}}{\pi} \{ & A r_1 V_2 \cos\theta + B\omega(\Delta L_1 V_2 \cos\theta - L_m V_1) \\ & - A\omega\Delta L_1 V_2 \sin\theta + B r_1 V_2 \sin\theta \} \end{aligned} \tag{20}$$

$$\begin{aligned} D = \frac{2\sqrt{2}}{\pi} \{ & A r_1 V_2 \sin\theta + A\omega(\Delta L_1 V_2 \cos\theta - L_m V_1) \\ & + B\omega\Delta L_1 V_2 \sin\theta - B r_1 V_2 \cos\theta \} \end{aligned} \tag{21}$$

$$\dot{i}_2 = -\frac{C + jD}{A^2 + B^2} \tag{22}$$

$$\begin{aligned} I_2 &= -\frac{C\cos\theta + D\sin\theta}{A^2 + B^2} \\ &= -\frac{1}{A^2 + B^2} \{ A r_1 V_2 + B\omega\Delta L_1 V_2 \\ &\quad - \omega L_m V_1 (A\sin\theta + B\cos\theta) \} \end{aligned} \tag{23}$$

When either the road side or the vehicle side, or both, are not in the resonant condition, the vehicle side does not achieve the synchronous rectification state by the proposed method. The vehicle side achieves a different state. The partial derivative of I_2 with respect to θ is described by the following equation.

$$\frac{\partial I_2}{\partial \theta} = \frac{\omega L_m V_1}{A^2 + B^2} (A\cos\theta - B\sin\theta) \tag{24}$$

Thus, I_2 is maximized when θ is:

$$\theta_{I_{2\max}} = \arctan\frac{A}{B} \tag{25}$$

Then, $I_{2\max}$ can be defined as:

$$I_{2\max} = -\frac{1}{A^2+B^2}(Ar_1V_2 + B\omega\Delta L_1 V_2 - \omega L_m V_1\sqrt{A^2+B^2}) \tag{26}$$

On the other hand, θ when the vehicle side is rectified by diodes is described in the following equation by the definition of θ in Table I and (23).

$$\begin{aligned}\angle v_2 &= \angle i_2 \\ \theta_{diode} &= \arctan\frac{D}{C}\end{aligned} \tag{27}$$

By substituting (23) into (27), $I_{2\mathrm{diode}}$ can be defined as:

$$I_{2\mathrm{diode}} = -\frac{1}{A^2+B^2}(Ar_1V_2 + B\omega\Delta L_1 V_2 + \omega L_m V_1\frac{AD+BC}{\sqrt{C^2+D^2}}) \tag{28}$$

Comparing $I_{2\max}$ and $I_{2\mathrm{diode}}$, the following equation can be obtained.

$$\begin{aligned}&I_{2\max} - I_{2\mathrm{diode}} \\ =&\frac{\omega L_m V_1}{(A^2+B^2)\sqrt{C^2+D^2}}\{\sqrt{(A^2+B^2)(C^2+D^2)} \\ &+ (AD+BD)\}\end{aligned} \tag{29}$$

If $AD+BD \geqq 0$, $I_{2\max} - I_{2\mathrm{diode}}$ is posihtive.

If $AD+BD < 0$, the positive and negative of (29) is judged by calculating the following.

$$\begin{aligned}&\sqrt{(A^2+B^2)(C^2+D^2)} + (AD+BD) \\ =&\frac{\sqrt{(A^2+B^2)(C^2+D^2)}^2 - (AD+BD)^2}{\sqrt{(A^2+B^2)(C^2+D^2)} - (AD+BD)} \\ =&\frac{(AC-BD)^2}{\sqrt{(A^2+B^2)(C^2+D^2)} - (AD+BD)} \\ \geqq&0\end{aligned} \tag{30}$$

Therefore, $I_{2\max} \geqq I_{2\mathrm{diode}}$ is valid for all $\Delta L_1, \Delta L_2$.

$I_{2\max} = I_{2\mathrm{diode}}$ is established when $AC = BD$. This is realized when:

$$(A^2+B^2)r_1V_2\cos\theta_{I_{2\max}} = 0 \tag{31}$$

One of the situation when (31) is realized is $\theta_{I_{2\max}} = 90°$. According to (25), this means $B = 0$. Thus, the following equation is realized.

$$r_1\Delta L_2 + r_2\Delta L_1 = 0 \tag{32}$$

This is also realized in the resonant condition when $\Delta L_1 = \Delta L_2 = 0$.

III. Implementation Method

The proposed method of the synchronous rectification is based on the method of the previous research [11]. The controller of the vehicle side changes θ to the positive or negative direction and measures I_2, and judges the direction where the optimal θ exists. In the conventional method, the width of the changed θ is fixed to 3°.

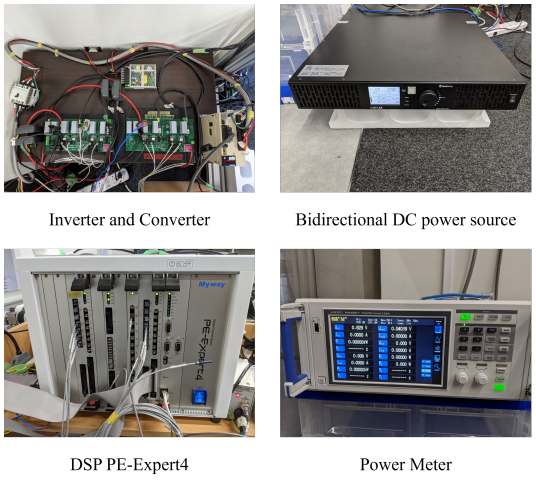

Fig. 3. Controller and measurement equipment.

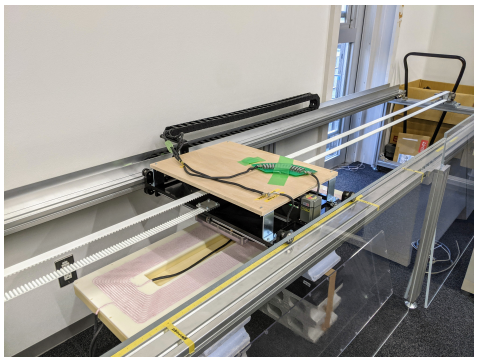

Fig. 4. Bench for experiment of D-WPT.

A. Gradient Descent Method

The proposed method is implemented in the following style. There are two important points when implementing the proposed method. One is the speed of the search for the optimal θ. The longer it takes to reach the optimal θ, the more losses occur on the vehicle side. The other is the stability of θ after θ settles into the optimal θ. If the θ fluctuates around the optimal θ, it also leads to losses.

To decide the width of the θ, the gradient descent is used. The algorithm is shown in Fig. 2. The previous values are needed to execute the cycle of this algorithm, so the initial setup is executed before the regular cycle. First, $\theta^{(0)}$ is set to 0°, and I_2 is measured as $I_2^{(0)}$. Then, the vehicle side adds $\theta_w^{(0)} = 3°$ to θ by changing the timing of switching, and waits $T^{(0)} = 1.25\,\mathrm{ms}$ for the transient response to settle down. The vehicle side measures I_2 as $I_2^{(1)}$, and this is the end of the initial setup. The regular cycle starts with $k = 2$. First, the vehicle side decide next $\theta_w^{(k)}$ by using $I_2^{(k-1)}$, $I_2^{(k-2)}$ and the previous $\theta_w^{(k-1)}$ based on the gradient descent. θ_w is decided by the following equation.

$$\theta_w^{(k)} = \alpha \times \frac{I_2^{(k-1)} - I_2^{(k-2)}}{\theta^{(k-1)} - \theta^{(k-2)}} \tag{33}$$

α is a constant parameter which effects the search speed and the settleness of θ. Then, the vehilce side adds $\theta_w^{(k)}$ to $\theta^{(k-1)}$,

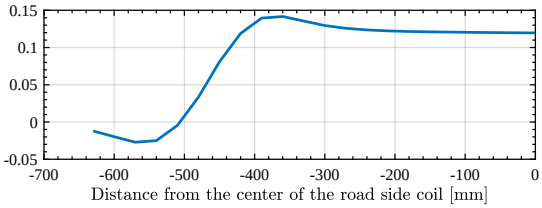

(a) Coupling coefficient k

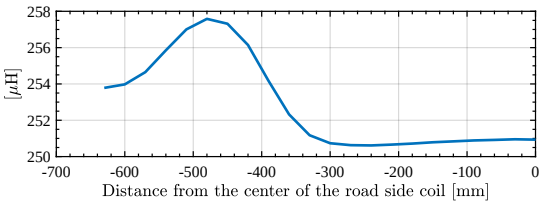

(b) Inductance of road side coil L_1

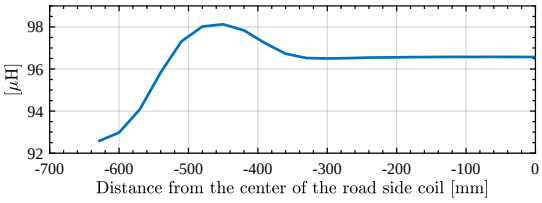

(c) Inductance of vehicle side coil L_2

Fig. 5. Coil parameters of this experiment at each position.

TABLE II
EFFICIENCY IN STOPPED STATE EXPERIMENT

efficiency(%)	$k = 0.12$ (x=0 mm)	$k = -0.025$ (x=−540 mm)
synchronous rectification	91.26	74.05
diode rectification	87.19	65.05

and measures DC received current I_2 after certain period T. T is the period to wait for the transient response to settle down. The larger θ_w becomes, the longer the settling time for waiting the transient response becomes. Thus, T is defined by the following equation. β is a parameter to determine the length of T.

$$T = 1250 \times |\theta_w|^{\beta} [\mu s] \tag{34}$$

After waiting T, the vehicle side measures I_2 as $I_2^{(k)}$. This is the end of the regular cycle. The vehicle side repeats this cycle endlessly to maximize the received DC current I_2.

B. Feedforward Additional Control

In a typical circular coil, L_m is negative when the central axes of the two facing coils are far apart, and positive when the central axes are coincident. Thus, L_m changes from negative to positive, and negative to positive when the vehicle moves. According to (11), I_2 is maximized when $\theta = 90°$ under the circumstances that L_m is positive. On the other hand, I_2 is maximized when $\theta = -90°$ under the circumstances that L_m is negative. Thus, it shortens the time of searching the optimal θ to change θ by $180°$ at the borderline where the positive and negative values of L_m change.

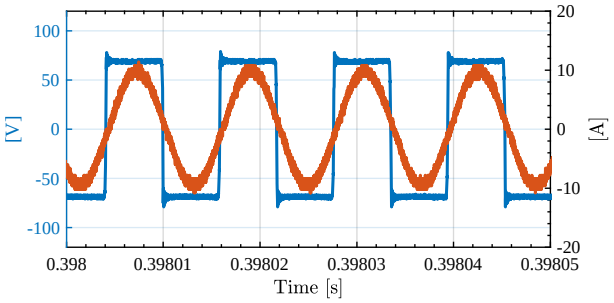

(a) AC waveform of the road side

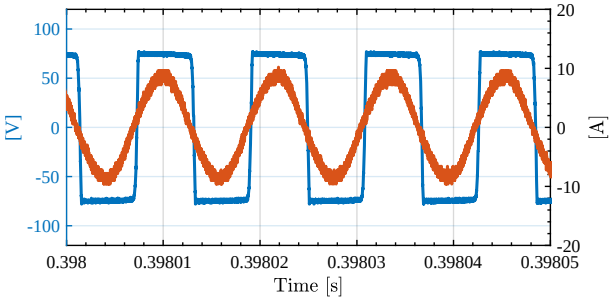

(b) AC waveform of the vehicle side

Fig. 6. AC waveform of the diode rectification in the stopped state experiment.

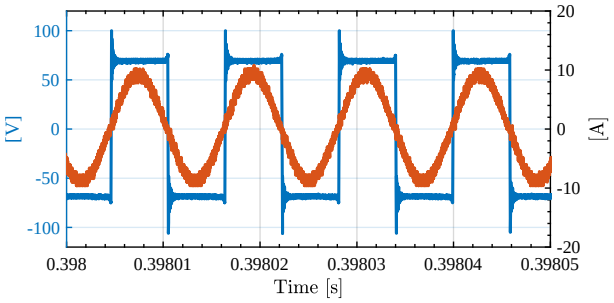

(a) AC waveform of the road side

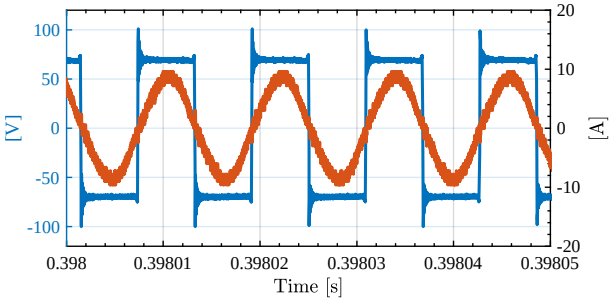

(b) AC waveform of the vehicle side

Fig. 7. AC waveform of the proposed synchronous rectification only with the DC current sensor in the stopped state experiment.

In the proposed algorithm, θ is temporarily stored at the end of the power supply section of the first negative coupling region. Then, at the beginning of the next power supply section where L_m is positive, the initial θ is set to the value that is obtained by adding $180°$ to the stored θ. The same process takes place at the boundary between the positive region and the latter negative region.

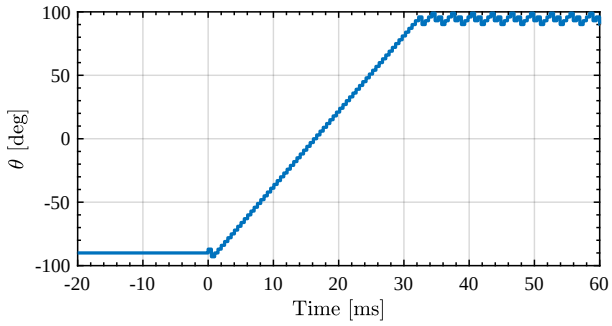

(a) Phase lead of $\dot{v}_2$ relative to $\dot{v}_1$

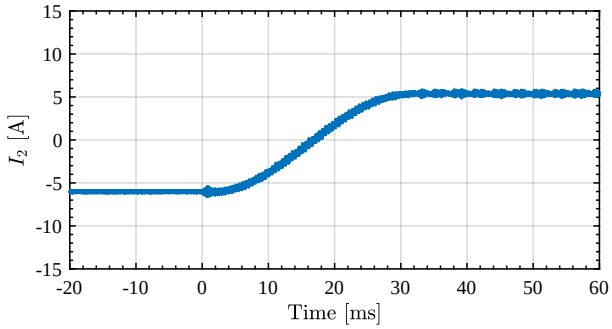

(b) Received DC current

Fig. 8. The optimal θ search speed for the conventional method in the stopped state.

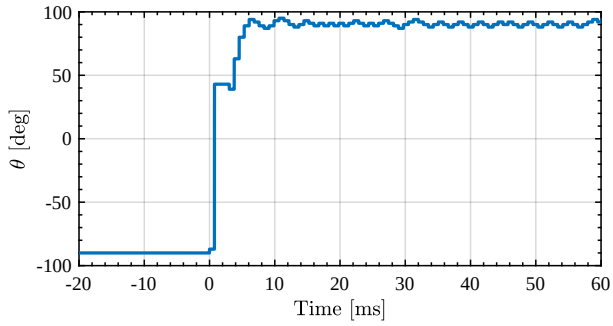

(a) Phase lead of $\dot{v}_2$ relative to $\dot{v}_1$

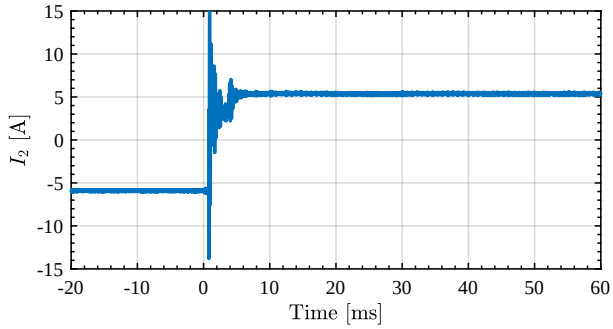

(b) Received DC current

Fig. 9. The optimal θ search speed for the proposed method in the stopped state.

IV. Experiment

The effect of the proposed method was verified in the experiment. The experimental equipment consists of a power supply, an inverter, coils, and a converter as shown in Fig. 3. A bench shown in Fig. 4 is used to move the vehicle side coil at a constant speed.

The coupling coefficient and the self inductances of the coils used in the experiments is shown in Fig. 5. The gap is $5\,\mathrm{cm}$. The coupling coefficient is positive when the vehicle side coil is on the road side coil. On the other hand, the coupling coefficient is negative when the vehicle side coil is on the side of the road side coil discussed in the previous section III-B. The distance from the center of the road side coil is defined as x, and $x = 0\,\mathrm{mm}$ in the nominal condition when the center of the vehicle side coil is just on the center of the road side coil.

A. Experiment in the Stopped State

The stopped state experiment was conducted to ensure the efficiency of the proposed method. First, the vehicle side coil is fixed at $x = 0\,\mathrm{mm}$. V_1 and V_2 are set at $70\,\mathrm{V}$. The diode rectifier is used for the comparison. The DC-DC efficiency at the steady-state is measured. It is defined as $\frac{V_2 I_2}{V_1 I_1}$.

The AC waveform of the conventional diode rectification is shown in Fig. 6, and the AC waveform of the synchronous rectification is shown in Fig. 7. The phases of the voltage and current in Fig. 7 are aligned as in the case of the diode rectification in Fig. 6, and the synchronous rectification is achieved.

The result of efficiency is shown in Table II. The efficiency of the proposed method is $91.26\,\%$, and $4.07\,\%$ higher than the diode rectifier. It means that the proposed method can reduce the loss by $31.77\,\%$ compared to the diode rectifier.

The efficiency is also measured at $x = -540\,\mathrm{mm}$, where L_m is negative and small, and L_1 and L_2 variate from the nominal values. L_m at this point is small compared to that at the center of the coil, so the efficiency is low in both the proposed method and the conventional diode rectifier. However, the efficiency of the proposed method is higher than that of the conventional method also in this negative coupling region.

The settling time of the conventional and the proposed method are compared. The optimal θ search speed for the conventional method is shown in Fig. 8. The conventional method changes θ by 3° to maximize I_2 [11]. The waiting time between the cycles is adjusted to be as short as possible, and set to $0.5\,\mathrm{ms}$. The optimal θ search speed for the proposed method is shown in Fig. 9. α of the proposed method is set to 150, and β is set to 0.2. The initial θ is set to -90° in both methods, which is the furthest value from the target value. The control algorithm starts from $0\,\mathrm{ms}$ in both method.

High peek currents flow at the start of the proposed method because θ changes dramatically. This is due to the transient response. According to the expanded AC waveform in Fig. 10, i_2 starts vibrating just after θ changes. However, although the proposed method flows some peak currents, it improves the search speed. The conventional method takes $32\,\mathrm{ms}$ to reach the target value, and the proposed method takes $8\,\mathrm{ms}$. The proposed method is 4 times faster than the conventional method.

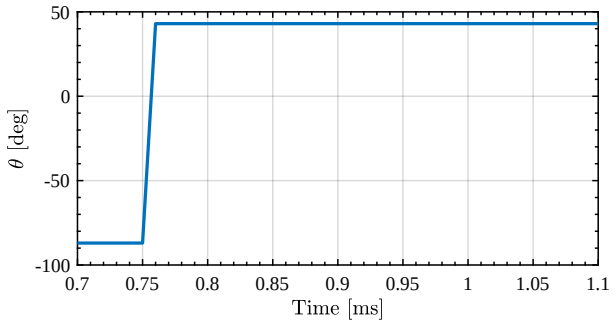

(a) Phase lead of $\dot{v}_2$ relative to $\dot{v}_1$

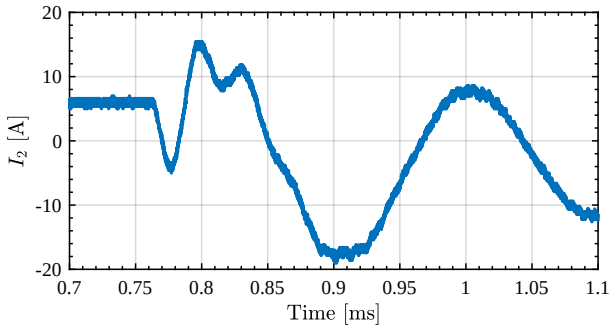

(b) Received DC current

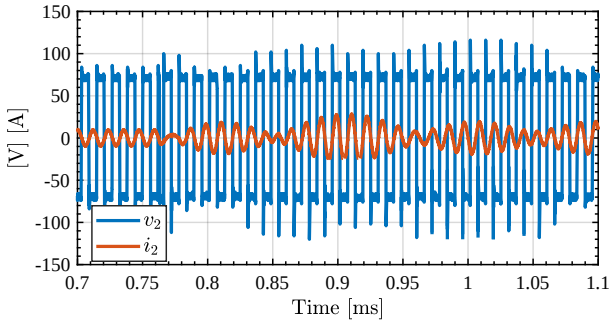

(c) v_2 and i_2

Fig. 10. The expanded waveform just after the start of the proposed method.

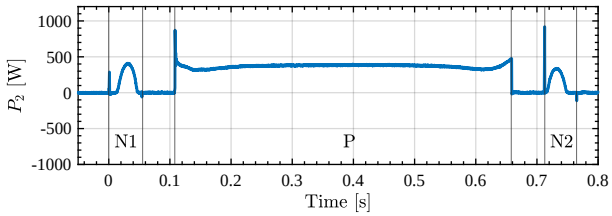

(a) received power P_2

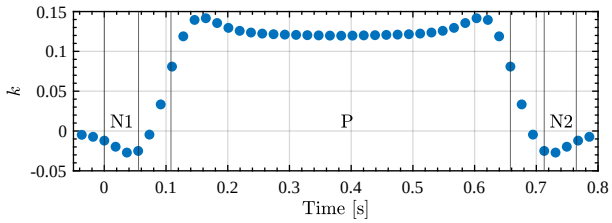

(b) coupling coefficient k

Fig. 11. The received power and the coupling coefficient in the diode rectification experiment.

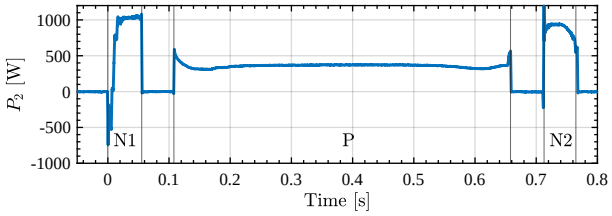

(a) received power P_2

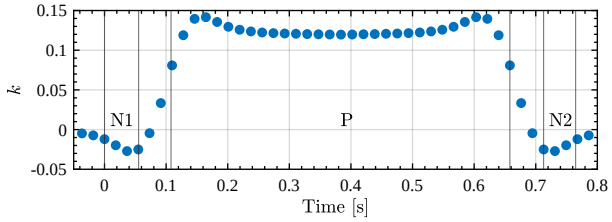

(b) coupling coefficient k

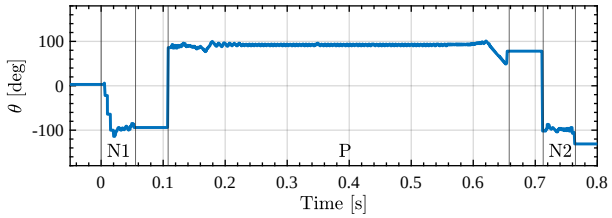

(c) Phase lead of $\dot{v}_2$ relative to $\dot{v}_1$

Fig. 12. The received power and the coupling coefficient in the synchronous rectification experiment.

B. Experiment in the Moving State

To verify the effectiveness of the proposed method under more practical conditions, the moving state experiment was conducted.

1) Experimental Condition: The road side coil is fixed, and the vehicle side coil is moved at $5\,\mathrm{km/h}$ by using the bench shown in Fig. 4. V_1 and V_2 are the same as the stoppoed condition at $70\,\mathrm{V}$. The diode rectifier is used for the comparison.

The road side coil transmits power both in the negative and positive coupling regions. The vehicle side can receive power both in the negative and positive regions. However, the vehicle side cannot receive power when the absolute of the coupling coefficient is near zero. The region is called the null region, and the road side does not transmit power in the region.

The road side starts to transmit power when $x = -630\,\mathrm{mm}$, and stops when $x = -540\,\mathrm{mm}$. This is the negative coupling region, and it is named the N1 region in this paper. Then the road side restarts to transmit power when $x = -450\,\mathrm{mm}$, and stops when $x = 450\,\mathrm{mm}$. This is the positive coupling region, and named the P region. The road side and vehicle side coils are symmetrical concerning the direction of travel, so the road side also transmits power between $x = 540\,\mathrm{mm}$ and $x = 630\,\mathrm{mm}$, which is another negative coupling region named the N2 region.

The controller of the vehicle side continuously runs the proposed algorithm described in Section III-A during receiving power and changes θ by 180° before and after the null region described in Section III-B.

TABLE III
RECEIVED POWER IN MOVING STATE EXPERIMENT

[W]	*N1*	*P*	*N2*	**Total**
synchronous rectification	42.2	198.0	45.9	286.0
diode rectification	9.2	202.8	7.4	219.5

TABLE IV
EFFICIENCY IN MOVING STATE EXPERIMENT

[%]	*N1*	*P*	*N2*	**Total**
synchronous rectification	59.3	90.8	68.2	80.3
diode rectification	23.3	88.0	21.7	72.1

2) The Result of the Experiment: The results of the experiments are shown in Fig. 11, 12. In the experiment of the proposed method, the initial value of the phase lead of $\dot{v}_2$ relative to $\dot{v}_1$ is set to $0°$, and it is not the synchronous rectification state. When the road side starts to transfer power at $0\,\mathrm{sec}$, the controller of the vehicle side starts to search the synchronous state point by the algorithm shown in Fig.2. The θ decreases because the θ is $-90°$ when the synchronous rectification is established. The received power P_2 is negative during the search, but the vehicle side can receive large power once the vehicle side achieves the synchronous rectification state. On the other hand, the amount of the received power of the conventional diode rectification is lower.

As the result, the received power of the proposed method is about 4.6 times larger than that of the conventional method in the N1 region as shown in Table III. The efficiency of the proposed method is also much higher than that of the conventional method as shown in Table IV. This is the advantage of the proposed method explained in section II-C that it can compensate for the decrease of the received power caused by the resonance shift.

Fig. 13 compares the received power by the diode rectification $P_{2\mathrm{diode}}$ and the received power by the proposed synchronous rectification $P_{2\mathrm{max}}$ in the calculation and the experiment. Fig. 13a shows the result calculated by (26), (28), and L_m in Fig. 5a–5c. $P_{2\mathrm{max}}$ and $P_{2\mathrm{diode}}$ are almost same around the center of the coils where ΔL_1 and ΔL_2 are almost 0. On the other hand, $P_{2\mathrm{max}}$ is larger than $P_{2\mathrm{diode}}$ around the edge of the coils, because certain ΔL_1 and ΔL_2 exist due to the effect of the ferrite. Fig. 13b compares $P_{2\mathrm{diode}}$ and $P_{2\mathrm{max}}$ in the experiment. It shows the same trend as the calculation result in Fig. 13a. The effectiveness of the proposed method that it can compensate the decreased received power caused by the deviation of the parameters is proved also in the experiment.

3) Effect on speedup: The vehicle side coil moves at $5\,\mathrm{km/h}$ in this experiment. The higher moving speed of vehicle side affects the algorithm of the proposed method. The proposed method monitors the change of I_2 when θ is changed. However, I_2 changes not only when θ changes, but also when L_m changes. It is needed that $\frac{\partial I_2}{\partial \theta}\Delta\theta$ is large compared to $\frac{\partial I_2}{\partial L_m}\Delta L_m$ for the proposed method to work properly. The maximum speed has been calculated at positive coupling region where the search is almost done. $\frac{\partial I_2}{\partial L_m}\Delta L_m$ in one cycle of the search is affected by the speed of the vehicle, and it has been calculated by the gradient of k in a region $420\,\mathrm{mm}$ wide from the coil center. $\Delta\theta$ can be adjusted by the controller. The larger $\Delta\theta$ is, the better the proposed method works even under faster conditions. When calculated in the condition of the experiment, $\frac{\partial I_2}{\partial \theta}\Delta\theta$ is larger than $\frac{\partial I_2}{\partial L_m}\Delta L_m$ if the speed of the vehicle is below $32\,\mathrm{km/h}$. The too small $\Delta\theta$ makes the proposed algorithm unstable as mentioned above, so the minimum $\Delta\theta$ is set to $3\,\mathrm{degrees}$ in the experiment. This means the minimum $\theta_w^{(k)}$ in Fig. 2 is limited to $3\,\mathrm{degrees}$. When the minimum $\Delta\theta$ is 1.5 times wider than the experimental condition, the maximum speed is increased to $72\,\mathrm{km/h}$.

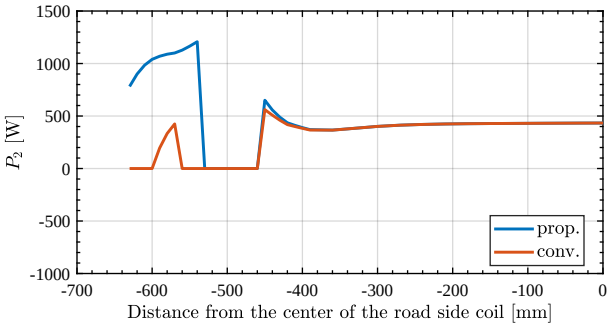

(a) P_2 calculated at each coil position

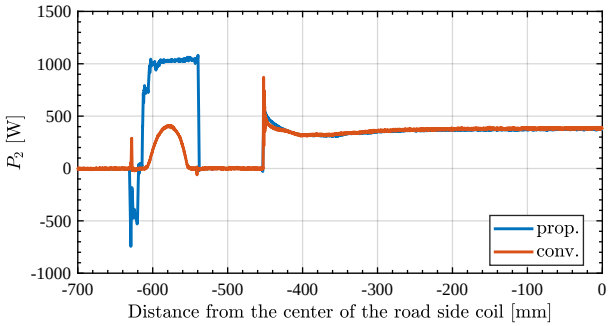

(b) P_2 actually measured in the experiment

Fig. 13. The comparison of the received power

V. CONCLUSION

A novel method that can increase the received power in WPT without AC current sensors was proposed in this paper. The method works differently for resonant and non-resonant conditions.

The principle of how the method works and the effects of the method are shown. In the resonant condition, it is revealed that the system ahieves the synchronous rectification state in the end by maximizing the vehicle side received DC current I_2. This makes the system more efficient compared to the diode rectification. In the non-resonant condition, the proposed method can compensate for the decrease of the received power caused by the resonance shift. This makes the vehicle side can receive more power.

The implementation method is also devised. To make the system settles into the best state of the power reception quickly, the gradient descent and the feedforward change of θ between the section are installed.

Then, the experiment that compares the proposed synchronous rectification and the conventional diode rectification was conducted. The experiments in the stopped state showed the proposed method can reduce the loss by 31.77 % and achieve the synchronous rectification 4 times faster. The experiments in the moving state showed the proposed method can receive 5.3 times more power in the negative coupling region where the parameters of the coils deviate.

ACKNOWLEDGMENT

This work was partly supported by JST-Mirai Program Grant Number JPMJMI21E2, JSPS KAKENHI Grant Number JP18H03768, JST CREST Grant Number JPMJCR15K3, JSPS KAKENHI Grant Number 19H02123.

REFERENCES

[1] S. Y. Hui, "Planar wireless charging technology for portable electronic products and Qi," *Proceedings of the IEEE*, vol. 101, no. 6, pp. 1290–1301, 2013.

[2] A. Kurs, A. Karalis, R. Moffatt, J. Joannopoulos, P. Fisher, and M. Soljacic, "Wireless power transfer via strongly coupled magnetic resonances.(RESEARCH ARTICLES)(Author abstract)," vol. 317, no. 5834, p. 83(4), 2007.

[3] F. Lu, H. Zhang, C. Zhu, L. Diao, M. Gong, W. Zhang, and C. C. Mi, "A Tightly Coupled Inductive Power Transfer System for Low-Voltage and High-Current Charging of Automatic Guided Vehicles," *IEEE Transactions on Industrial Electronics*, vol. 66, no. 9, pp. 6867–6875, 2019.

[4] J. P. Sampath, D. M. Vilathgamuwa, and A. Alphones, "Efficiency Enhancement for Dynamic Wireless Power Transfer System with Segmented Transmitter Array," *IEEE Transactions on Transportation Electrification*, vol. 2, no. 1, pp. 76–85, 2016.

[5] P. K. S. Jayathurathnage, A. Alphones, D. M. Vilathgamuwa, and A. Ong, "Optimum Transmitter Current Distribution for Dynamic Wireless Power Transfer with Segmented Array," *IEEE Transactions on Microwave Theory and Techniques*, vol. 66, no. 1, pp. 346–356, 2018.

[6] I. S. Suh and J. Kim, "Electric vehicle on-road dynamic charging system with wireless power transfer technology," *Proceedings of the 2013 IEEE International Electric Machines and Drives Conference, IEMDC 2013*, pp. 234–240, 2013.

[7] H. Fujimoto, O. Shimizu, S. Nagai, T. Fujita, D. Gunji, and Y. Ohmori, "Development of wireless in-wheel motors for dynamic charging: From 2nd to 3rd generation," *2020 IEEE PELS Workshop on Emerging Technologies: Wireless Power Transfer, WoW 2020*, pp. 56–61, 2020.

[8] F. Liu, W. Lei, T. Wang, C. Nie, and Y. Wang, "A phase-shift soft-switching control strategy for dual active wireless power transfer system," *2017 IEEE Energy Conversion Congress and Exposition, ECCE 2017*, vol. 2017-January, pp. 2573–2578, 2017.

[9] A. Konishi, K. Umetani, and E. Hiraki, "High-frequency Self-Driven Synchronous Rectifier Controller for WPT Systems," *2018 International Power Electronics Conference, IPEC-Niigata - ECCE Asia 2018*, pp. 1602–1609, 2018.

[10] D. Tajima, O. Shimizu, and H. Fujimoto, "High-Efficiency Operation of Wireless In-Wheel Motor at Low Load Using Intermittent Synchronous Rectification with Improved Transient Stability," *IECON (Industrial Electronics Conference)*, vol. 2019-October, pp. 1089–1094, 2019.

[11] D. Shirasaki and H. Fujimoto, "Novel Synchronous Rectification Method for WPT Only by DC Current Sensor," in *2021 IEEE PELS Workshop on Emerging Technologies: Wireless Power Transfer (WoW)*, 2021, pp. 1–5.

[12] R. Althomali and M. Alsumiri, "Improved mppt controllers for wind generation system based on hill climbing technique," in *2017 Intl Conf on Advanced Control Circuits Systems (ACCS) Systems 2017 Intl Conf on New Paradigms in Electronics Information Technology (PEIT)*, 2017, pp. 140–143.

[13] M. Albach, A. Stadler, and M. Spang, "The Influence of Ferrite Characteristics on the Inductance of Coils With Rod Cores," *IEEE Transactions on Magnetics*, vol. 43, no. 6, pp. 2618–2620, 2007.

[14] A. Desmoort, O. Deblecker, and Z. De Greve, "Active Rectification For the Optimal Command of Bidirectional Resonant Wireless Power Transfer Robust to Severe Circuit Parameters Deviations," *IEEE Transactions on Industry Applications*, vol. 56, no. 2, pp. 1640–1648, 2020.

[15] C. Liu, D. J. Thrimawithana, G. A. Covic, and M. Kesler, "Active impedance control for inductive charging of electric vehicles," in *2020 IEEE PELS Workshop on Emerging Technologies: Wireless Power Transfer (WoW)*, 2020, pp. 16–20.

[16] S. Ann and B. K. Lee, "Analysis of Impedance Tuning Control and Synchronous Switching Technique for a Semibridgeless Active Rectifier in Inductive Power Transfer Systems for Electric Vehicles," *IEEE Transactions on Power Electronics*, vol. 36, no. 8, pp. 8786–8798, 2021.

[17] R. Matsumoto, B. Ji, H. Fujimoto, and Y. Hori, "Resonance Frequency Adjustment Using PWM-Controlled Variable Capacitor for In-Motion WPT with Circuit Parameter Deviations," in *2020 IEEE PELS Workshop on Emerging Technologies: Wireless Power Transfer (WoW)*, 2020, pp. 158–163.

[18] D.-H. Kim and D. Ahn, "Self-Tuning LCC Inverter Using PWM-Controlled Switched Capacitor for Inductive Wireless Power Transfer," *IEEE Transactions on Industrial Electronics*, vol. 66, no. 5, pp. 3983–3992, 2019.

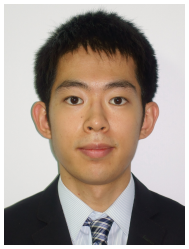

Daisuke Shirasaki received his B.E. degree from the Department of Electrical and Electronic Engineering, the University of Tokyo, Japan in 2020. He is currently working toward an M.S. degree at the Department of Advanced Energy, Graduate School of Frontier Sciences, the University of Tokyo. His interests are in dynamic wireless power transfer for EVs. He is a student member of the Institute of Electrical and Electronics Engineers.

Toshiyuki Fujita received a B.S. degree in electrical engineering, an M.S. degree in physical electronics, and a Ph.D degree in electrical and electronic engineering from the Tokyo Institute of Technology, Tokyo, Japan, in 2008, 2010, and 2017, respectively. Since 2014, he has been with Technova Inc., Tokyo. He worked for Panasonic Corporation, Osaka, Japan from 2010 to 2014. In 2019, he joined the University of Tokyo, Chiba, Japan, as a project assistant professor. His research interests include WPT systems for electric vehicles, ac/dc converters, and its control methods. He is a member of IEE Japan, the Society of Automotive Engineers of Japan, and the Japan Society of Applied Physics.

Hiroshi Fujimoto received the Ph.D. degree in the Department of Electrical Engineering from the University of Tokyo in 2001.In 2001, he joined the Department of Electrical Engineering, Nagaoka University of Technology, Niigata, Japan, as a research associate. From 2002 to 2003, he was a visiting scholar in the School of Mechanical Engineering, Purdue University, U.S.A. In 2004, he joined the Department of Electrical and Computer Engineering, Yokohama National University, Yokohama, Japan, as a lecturer and he became an associate professor in 2005. He is currently a professor of the University of Tokyo since 2021. He received the Best Paper Awards from the IEEE Transactions on Industrial Electronics in 2001 and 2013, Isao Takahashi Power Electronics Award in 2010, and Best Author Prize of SICE in 2010. His interests are in control engineering, motion control, nano-scale servo systems, electric vehicle control, and motor drive. He is a senior member of IEE of Japan and IEEE. He is also a member of the Society of Instrument and Control Engineers, the Robotics Society of Japan, and the Society of Automotive Engineers of Japan.